# Momentum-Space Correlations of a One-Dimensional Bose Gas

Bess Fang,[1] Aisling Johnson,[1] Tommaso Roscilde,[2,3] and Isabelle Bouchoule[1]
[1]*Laboratoire Charles Fabry, CNRS UMR 8501, Institut d'Optique, Université Paris Sud 11, 2 Avenue Augustin Fresnel, 91127 Palaiseau, France*
[2]*Laboratoire de Physique, CNRS UMR 5672, Ecole Normale Supérieure de Lyon, Université de Lyon, 46 Allée d'Italie, Lyon F-69364, France*
[3]*Institut Universitaire de France, 103 boulevard Saint-Michel, 75005 Paris, France*
(Received 13 May 2015; published 2 February 2016)

Analyzing the noise in the momentum profiles of single realizations of one-dimensional Bose gases, we present the experimental measurement of the full momentum-space density correlations $\langle \delta n_p \delta n_{p'} \rangle$, which are related to the two-body momentum correlation function. Our data span the weakly interacting region of the phase diagram, going from the ideal Bose gas regime to the quasicondensate regime. We show experimentally that the bunching phenomenon, which manifests itself as super-Poissonian local fluctuations in momentum space, is present in all regimes. The quasicondensate regime is, however, characterized by the presence of negative correlations between different momenta, in contrast to the Bogolyubov theory for Bose condensates, predicting positive correlations between opposite momenta. Our data are in good agreement with *ab initio* calculations.

DOI: 10.1103/PhysRevLett.116.050402

*Introduction.*—Ultracold-atom experiments have proven their efficiency as quantum simulators of models in quantum many-body physics [1]. One dimensional (1D) gases, in particular, are accurately simulated, as shown by the excellent agreement between experimental results and *ab initio* theoretical predictions [2–9]. Among the least understood properties of quantum many-body systems is the out-of-equilibrium dynamics, addressed recently by several cold-atom experiments [8,10–12].

Correlation functions are essential tools used to describe the physics of a system, as they fundamentally characterize the different phases the system can exhibit [13]. This is particularly true for 1D gases, where the role of fluctuations is enhanced. For instance, the local two-body correlation function in real space distinguishes the ideal Bose gas (IBG) regime (characterized by bunching) from the quasi Bose-Einstein condensate (QBEC) regime (with the absence of bunching) from the fermionized regime (characterized by strong antibunching) [7,14]. The two-body correlation function in an expanding Bose gas has been measured in [15] and can be used for thermometry in the QBEC regime [16], while higher order correlation functions allow the identification of nonthermal states [17]. Correlation functions are also essential to describe out-of-equilibrium dynamics. For example, the light-cone effect has been reported on the time evolution of the correlation functions after a sudden perturbation of the system [10,11], and the dynamical Casimir effect was identified by studying a two-body correlation function in [18]. Investigating the behavior of correlation functions is thus an important issue in quantum simulation. However, correlation functions, especially those of higher orders, are in general unknown theoretically, not even at thermal equilibrium, so that further knowledge in this domain is highly desirable.

In this Letter, we investigate for the first time the full structure of the second-order correlation function in momentum space of a 1D Bose gas at thermal equilibrium. The measurements rely on the statistical noise analysis of sets of momentum profiles taken under similar experimental conditions. Our data span the weakly interacting region of the phase diagram of 1D Bose gases [19], going from the QBEC regime to the IBG regime. The bunching phenomenon, which manifests itself by strong, super-Poissonian local fluctuations in momentum space, is seen in all regimes. The QBEC regime is, however, characterized by the presence of negative correlations associating different momenta, as predicted in [20]. This contrasts with the positive correlations between opposite momenta expected for systems with true or quasi-long-range order [21]. In both asymptotic regimes, our data compare well with appropriate models, while the data in the crossover are in good agreement with quantum Monte Carlo (QMC) simulations. These comparisons involve no fitting parameters. Finally, we propose a quantitative criterion to characterize the crossover.

*Experiment.*—Using an atom-chip experiment, we realize single quasi-1D ultracold $^{87}$Rb clouds, as described in [22]. Using evaporative cooling, we prepare atoms in the $|F = 2, m_F = 2\rangle$ ground state, at thermal equilibrium in a harmonic trap whose transverse and longitudinal oscillation frequencies are $\omega_\perp/(2\pi) \simeq 1.9$ kHz and $\omega_z/(2\pi) \simeq 7$ Hz, respectively. The estimated population in the transverse excited states is at most 40%, such that the data are indeed close to the 1D regime of Bose gases. We perform

 

thermometry by fitting the measured mean *in situ* linear density profile $\rho(z)$ and density fluctuations to the thermodynamic predictions of the modified Yang-Yang model [2,4], where the interatomic interaction is taken into account only in the transverse ground state, modeled by a contact term of coupling constant $g = 2\hbar\omega_\perp a$, $a = 5.3$ nm being the 3D scattering length.

A single shot of the momentum distribution $n(p)$ is obtained by imaging the atomic cloud in the Fourier plane of a magnetic lens using the focusing technique [22–24], as detailed in the Supplemental Material [25]. The spatial distribution of the atom cloud then reflects the initial momentum distribution [22]. These images are discretized with a pixel size in momentum space $\Delta$. Moreover, the resolution of the optical system and the atomic motion during the imaging pulse are responsible for blurring, modeled by a Gaussian impulse response function of root-mean-square width $\delta$. The effective atom number measured in pixel $\alpha$ is thus $N_\alpha = \int dp n(p)\mathcal{A}(\alpha, p)$, where $\mathcal{A}(\alpha, p) = \int_{\Delta_\alpha} dq e^{-(p-q)^2/(2\delta^2)}/(\delta\sqrt{2\pi})$. The second-order correlation function is deduced from a set of momentum profiles taken under similar experimental conditions. The standard deviation of shot-to-shot atom-number fluctuations ranges from 4% at high densities to 40% at low densities. To mitigate their effect, we order profiles according to their atom number and, for each profile, we use a running average to compute the corresponding mean profile $\langle N_\alpha \rangle$. Moreover, we normalize each profile to the atom number of the running average, before computing the fluctuations $\delta N_\alpha = N_\alpha - \langle N_\alpha \rangle$. We finally extract the momentum-correlation map $\langle \delta N_\alpha \delta N_\beta \rangle$. Figure 1 (top row) shows the results for three different clouds lying, respectively, (A) in the IBG regime, (B) in the QBEC-IBG crossover, and (C) deep in the QBEC regime. For the data presented in this Letter, the focusing time is $\tau = 25$ ms, leading to a pixel size in momentum space $\Delta/\hbar = 0.15\ \mu\text{m}^{-1}$. The resolution is $\delta/\Delta \simeq 1.1$ [28].

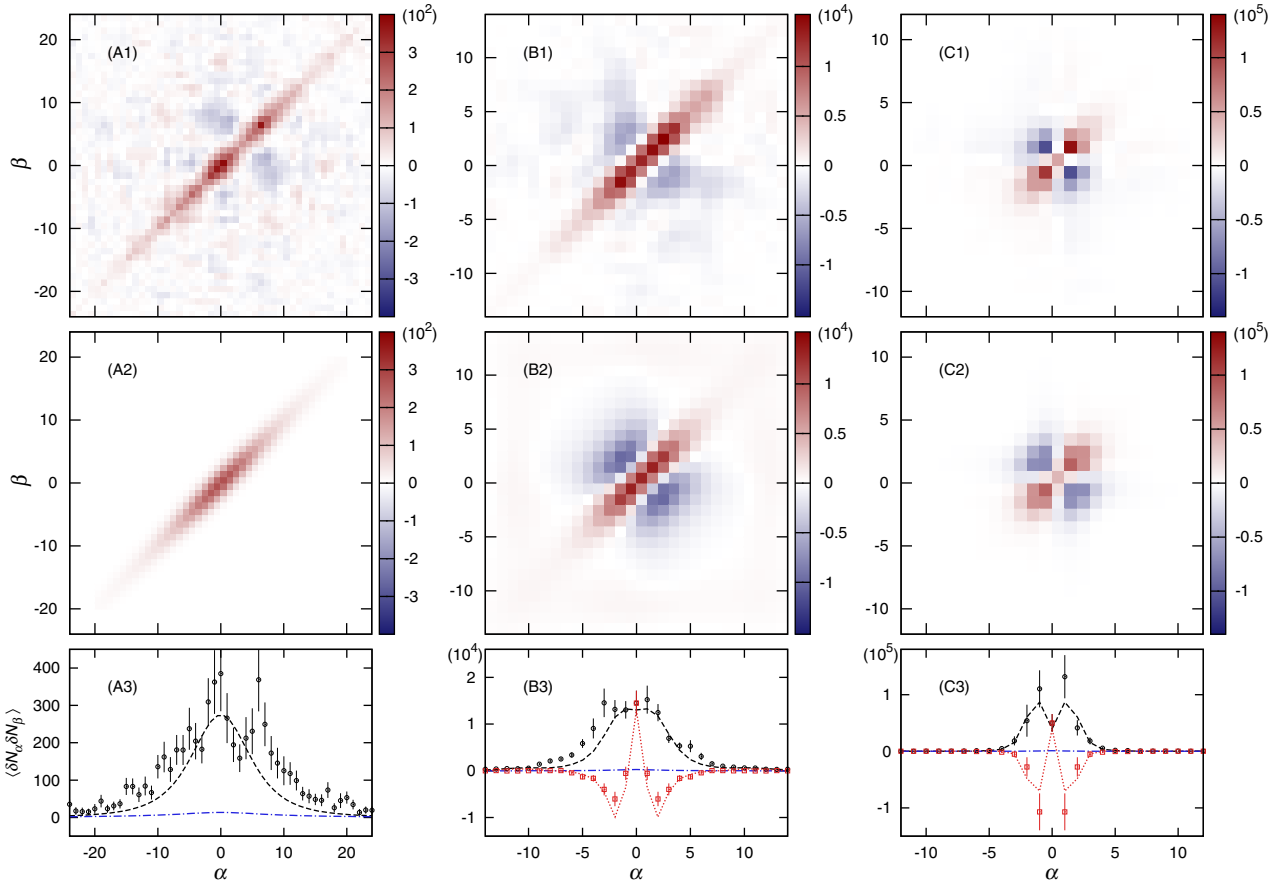


FIG. 1. Momentum correlations $\langle \delta N_\alpha \delta N_\beta \rangle$ for a gas in the IBG regime (data A, left column), in the QBEC regime (data C, right column), and in the QBEC-IBG crossover (data B, middle column). The pixel size is $\Delta/\hbar = 0.15\ \mu\text{m}^{-1}$. The experimental data are shown in the top row. Data A, B, and C are compared with the IBG theory, QMC calculations, and QBEC theory, respectively, at the temperature of the data determined by independent thermometry methods [25]. The middle row gives the computed momentum correlations. The bottom row shows the diagonal cuts: the experimental data in circles for $\alpha = \beta$ (squares for $\alpha = -\beta$ for data B and C only) are compared with their respective theory model in dashed (dotted) lines. The error bars are statistical. The dash-dotted lines give the shot-noise limit.

*Ideal Bose gas regime.*—Thermometry based on *in situ* density profiles indicates that data A lie within the IBG regime ($N = 1900$, $T = 109$ nK) [25]. Figure 1 (A1) shows the corresponding momentum correlations. We observe large correlations on the diagonal $\alpha \simeq \beta$, while $\langle \delta N_\alpha \delta N_\beta \rangle$ takes substantially smaller and rather erratic values in the rest of the plane [29]. This is consistent with what is expected for a homogeneous IBG in the grand canonical ensemble: since the single-particle eigenstates have well defined momenta, the correlations between different momenta are vanishing. Moreover, fluctuations of the occupation number $N_p$ in the state of momentum $p$ are $\langle \delta N_p^2 \rangle = \langle N_p \rangle + \langle N_p \rangle^2$, where the second term is the famous bunching term. Previous results generalize to the case of our trapped clouds through a local density approximation (LDA), as outlined in the Supplemental Material [25], valid since the correlation length of $\langle \psi^\dagger(z)\psi(z') \rangle$ is much smaller than the cloud length $L$ [30]. The momentum-space density correlations are then the sum of the shot-noise and bunching contributions,

$$\langle \delta n_p \delta n_{p'} \rangle = \delta(p - p') \langle n_p \rangle + B(p, p'),$$
$$B(p, p') = \left| \int dz \langle \nu^{(h)}_{\rho(z),T}[(p + p')/2] \rangle e^{i(p-p')z/\hbar} \right|^2, \quad (1)$$

where the bunching term $B(p, p')$ uses the momentum distribution $\nu^{(h)}_{\rho,T}(p)$ of a homogeneous gas of temperature $T$ and linear density $\rho$, normalized to $\rho = \int dp \nu^{(h)}_{\rho,T}(p)$. $B(p, p')$ takes nonzero values only for $|p' - p|$ of the order of $\hbar/L$. Since here $\hbar/L \ll \delta$, one can make the approximation $B(p, p') = \mathcal{B}(p)\delta(p - p')$, where

$$\mathcal{B}(p) = 2\pi\hbar \int dz \langle \nu^{(h)}_{\rho(z),T}(p) \rangle^2. \quad (2)$$

Note that for a degenerate cloud, for $p$ within the width of $n(p)$, the bunching term is much larger than the shot-noise term since $\langle \nu^{(h)}_{\rho(z),T}(p) \rangle \gg 1$. Finally, blurring and discretization lead to the momentum-correlation map

$$\langle \delta N_\alpha \delta N_\beta \rangle = \int\int dp dp' \mathcal{A}(\alpha, p)\mathcal{A}(\beta, p') \langle \delta n_p \delta n_{p'} \rangle. \quad (3)$$

The theoretical prediction quantitatively describes our measurements, as shown in Fig. 1 (A1–A2). Here, we evaluate Eq. (2) approximating $\langle \nu^{(h)}_{\rho(z),T}(p) \rangle$ by its value for highly degenerate IBG gases: a Lorentzian of full width at half maximum (FWHM) of $2\hbar/l_\phi$, where $l_\phi = \hbar^2\rho/(mk_BT)$. Since correlations between different pixels are introduced by the finite resolution alone [31], the only relevant information is the diagonal term $\langle \delta N_\alpha^2 \rangle$, whose scaling behavior is discussed in the Supplemental Material [25]. In Fig. 1 (A3), we overlay the measured $\langle \delta N_\alpha^2 \rangle$ to theoretical predictions, and find a good agreement up to statistical error of the measurement. The fluctuations are well above the shot-noise level, which is obtained by setting $\mathcal{B}(p) = 0$, showing that this IBG is highly degenerate.

Note that the above grand-canonical analysis is legitimate since $\hbar/l_\phi \gg \Delta \gg \hbar/L$: a pixel may be described by a subsystem at equilibrium with the reservoir of energy and particles formed by the rest of the cloud.

*Quasicondensate regime.*—The analysis of the *in situ* density fluctuations [25] shows that data C lie in the QBEC regime ($N = 14000$, $T \simeq 75$ nK). The mean density profile indicates a slightly higher temperature ($T = 103$ nK), the difference possibly coming from a deviation from the Gibbs ensemble [12,17]. We show the measured momentum correlations in Fig. 1 (C1) and its diagonal cuts along $\alpha = \beta$ and $\alpha = -\beta$ in (C3). We first observe that a strong bunching in momentum space is also present here: the measured $\langle \delta N_\alpha^2 \rangle$ is well above the shot-noise level alone. This is in stark contrast with the behavior in real space, where the QBEC regime is characterized by the suppression of the bosonic bunching [32]. Moreover, the correlation map $\langle \delta N_\alpha \delta N_\beta \rangle$ shows strong anticorrelations around the region $\alpha = -\beta$ (i.e., $p' = -p$). These features are characteristic of the QBEC regime in a grand canonical ensemble, and have been computed for a homogeneous gas in [20]. Since the correlation length of the gas is much smaller than $L$ [33], LDA applies and, as shown in the Supplemental Material [25], we have

$$\langle \delta n_p \delta n_{p'} \rangle \simeq \delta(p - p') \langle n_p \rangle + B(p, p') + \langle \delta n_p \delta n_{p'} \rangle_{\text{reg}}, \quad (4)$$

$$\langle \delta n_p \delta n_{p'} \rangle_{\text{reg}} = \int dz \frac{l_\phi(z)^3 \rho(z)^2}{(2\pi\hbar)^2} \mathcal{F}\left( \frac{2l_\phi(z)p}{\hbar}, \frac{2l_\phi(z)p'}{\hbar} \right), \quad (5)$$

where $\mathcal{F}$ is the dimensionless function given by Eq. (29) of [20], and $B(p, p')$ is evaluated substituting $\nu^{(h)}_{\rho,T}(p)$ by a Lorentzian function of FWHM $\hbar/l_\phi$. The effect of the finite resolution and pixelization is taken into account using Eq. (3). These predictions, plotted in Fig. 1 (C2—C3), are in quantitative agreement with the experimental data. Note that the center-of-mass (COM) motion is decoupled from the internal degrees of freedom in a harmonic trap, and the COM fluctuations are about twice as large as those expected at thermal equilibrium for this data set [34]. To mitigate their effect, we postselect the data by bounding the COM fluctuations. Moreover, since the experimental resolution is not sufficient to resolve momentum scales of the order of $\hbar/l_\phi$, the effect of $\langle \delta n_p \delta n_{p'} \rangle_{\text{reg}}$ on the diagonal reduces the signal that would be expected from bunching alone by almost a factor of 10.

Our results provide the first experimental proof of the persistence of bunching in momentum space in a QBEC, as

well as the presence of negative correlations, in particular between opposite momenta. The latter contrasts with the behavior expected for a weakly interacting Bose-Einstein condensate, where Bogoliubov theory predicts the presence of positive correlations between opposite momenta [25]. The absence of opposite-$p$ positive correlations is a clear consequence of the absence of true long range order.

The atom-number fluctuations are strongly reduced in a QBEC because of repulsive interactions, and the negative part of $\mathcal{F}$, which concentrates on the momentum region $p \lesssim \hbar/l_c$, enforces the reduced atom-number fluctuations by compensating for the diagonal bunching term [20]. In our experiment, however, one may *a priori* suspect that the measured anticorrelations could come from the normalization procedure used in the data analysis. We rule out such a possibility by performing several checks, detailed in the Supplemental Material [25]. The agreement with theory in our case is ensured by the fact that the fluctuations $\langle \delta n_p \delta n_{p'} \rangle_{\mathrm{reg}}$ are dominated by the contribution from the central part of the cloud, where $l_\phi$ is the largest [see Eq. (5)]. It is well described by the grand canonical ensemble as the rest of the cloud acts as a reservoir, and the corresponding anticorrelations are much stronger than those introduced by the normalization of the total atom number. The negative part of the correlation map thus reflects a local decrease of the atom-number fluctuations.

*In the QBEC-IBG crossover.*—While the theoretical analyses above describe reasonably well the two asymptotic regimes of IBG and QBEC, they do not permit us to investigate the crossover in between. To explore the crossover, we use canonical QMC calculations [35]. Discretizing space allows us to recast the Lieb-Liniger model in the form of a Bose-Hubbard model [22], which can be simulated via the stochastic series expansion with directed-loop updates [36]. In particular, a double directed-loop update allows one to compute the momentum correlations $\langle \delta n_p \delta n_{p'} \rangle$. Blurring and pixelization is then applied according to Eq. (3). The features of $\langle \delta n_p \delta n_{p'} \rangle$ are mainly washed out at the level of the experimental resolution [37], demanding a very high numerical precision on $\langle \delta n_p \delta n_{p'} \rangle$ to properly evaluate the discretized correlation map. The results for the parameters of data B ($N = 7000$, $T = 144$ nK), shown in Fig. 1 (B2) and (B3), reproduce quantitatively the features seen in the experimental data, shown in Fig. 1 (B1) and (B3). Namely, the bunching phenomenon remains prominent on the $\alpha = \beta$ diagonal, while the anticorrelations along the $\alpha = -\beta$ is less pronounced than what is found for data C.

*Quantifying the crossover.*—As shown in the Supplemental Material [25], Eqs. (4) and (5) generalize the computation of the momentum correlations to the whole parameter space, provided $\mathcal{F}$ is now a function of the reduced temperature $t = 2\hbar^2 k_B T/(mg^2)$ and the interaction parameter $\gamma(z) = mg/[\hbar^2 \rho(z)]$. $\mathcal{F}$ interpolates between 0 in the IBG regime ($t \gg 1$ and $t\gamma^{3/2} \gg 1$) and Eq. (29) of [20] in the QBEC regime ($t\gamma^{3/2} \ll 1$ and $\gamma \ll 1$). For the experimental resolution of this Letter, however, one cannot isolate the contribution of $\mathcal{F}$ from that of the bunching term. We thus consider the experimental quantity

$$C = \sum_\alpha \langle \delta N_\alpha \delta N_{-\alpha} \rangle / \langle N_0 \rangle. \tag{6}$$

As derived in the Supplemental Material [25], in the limit $\delta, \Delta \ll \hbar/l_\phi$ and $\delta \gg \Delta$, $C$ depends only on $t$ and $\gamma_0 \equiv \gamma$ ($z = 0$). For a highly degenerate IBG, we find $C \simeq 1.08/(t\gamma_0^2)$, whereas $C \simeq -2.28/(t\gamma_0^2)$ for a QBEC. These asymptotic behaviors are shown as dashed and dotted lines in Fig. 2. The solid line gives the prediction for an IBG (where $Ct\gamma_0^2$ now depends on $t$ and $\gamma_0$) at $t = 1000$ [38]. Figure 2 also displays the experimental values of $Ct\gamma_0^2$ for data A–C. However, since $\hbar/l_\phi \gg \delta \gg \Delta$ is not satisfied for our data sets, the above theoretical predictions are not expected to quantitatively agree with the experimental data. Moreover, comparing different data sets is delicate since they correspond to different values of $\delta/l_\phi$.

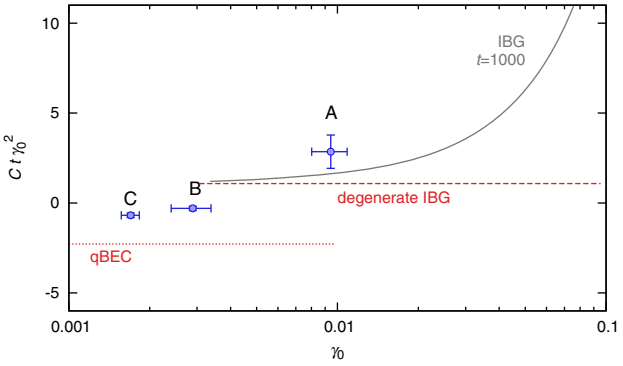


FIG. 2. $Ct\gamma_0^2$ versus $\gamma_0$, the interaction parameter at the center of the cloud. The theoretical predictions in the limit $\hbar/l_\phi \gg \delta \gg \Delta$ [25] are plotted for highly degenerate IBG (dashed line), QBEC (dotted line), and IBG (solid line, computed at $t = 1000$). Circles are experimental results for data A–C (corresponding to $t = 1170$, 1760, 920). The error bars account for both fitting (in $t$) and statistics (in $C$ and $\gamma_0$).

*Outlook.*—A future extension of our study of two-body correlations in momentum space concerns the fermionized regime of 1D Bose gases, where quantum fluctuations, difficult to observe in momentum space for weakly interacting gases, might have measurable effects. The study of correlations in momentum space at thermal equilibrium could serve as a reference for the investigation of nonthermal states and that of out-of-equilibrium dynamics arising, for example, from a quench of the coupling constant $g$. Correlations in momentum space have also been proposed as a probe of Hawking-like radiation generated by a sonic black hole [39], and the results of this Letter are certainly relevant for this quest.

This work has been supported by Cnano IdF and by the Austro-French FWR-ANR Project No. I607. T. R. acknowledges support of the ANR ("ArtiQ" project). QMC simulations have been performed on the PSMN cluster (ENS Lyon).

[1] I. Bloch, J. Dalibard, and W. Zwerger, Rev. Mod. Phys. **80**, 885 (2008).
[2] J. Armijo, T. Jacqmin, K. Kheruntsyan, and I. Bouchoule, Phys. Rev. A **83**, 021605 (2011).
[3] T. Jacqmin, J. Armijo, T. Berrada, K. V. Kheruntsyan, and I. Bouchoule, Phys. Rev. Lett. **106**, 230405 (2011).
[4] A. H. van Amerongen, J. J. P. van Es, P. Wicke, K. V. Kheruntsyan, and N. J. van Druten, Phys. Rev. Lett. **100**, 090402 (2008).
[5] B. Paredes, A. Widera, V. Murg, O. Mandel, S. Fölling, I. Cirac, G. V. S. T. W. Hänsch, and I. Bloch, Nature (London) **429**, 277 (2004).
[6] T. Kinoshita, T. Wenger, and D. S. Weiss, Science **305**, 1125 (2004).
[7] T. Kinoshita, T. Wenger, and D. S. Weiss, Phys. Rev. Lett. **95**, 190406 (2005).
[8] T. Kinoshita, T. Wenger, and D. Weiss, Nature (London) **440**, 900 (2006).
[9] E. Haller, R. Hart, M. J. Mark, J. G. Danzl, L. Reichsöllner, M. Gustavsson, M. Dalmonte, G. Pupillo, and H.-C. Nägerl, Nature (London) **466**, 597 (2010).
[10] M. Cheneau, P. Barmettler, D. Poletti, M. Endres, P. Schau, T. Fukuhara, C. Gross, I. Bloch, C. Kollath, and S. Kuhr, Nature (London) **481**, 484 (2012).
[11] T. Langen, R. Geiger, M. Kuhnert, B. Rauer, and J. Schmiedmayer, Nat. Phys. **9**, 640 (2013).
[12] B. Fang, G. Carleo, A. Johnson, and I. Bouchoule, Phys. Rev. Lett. **113**, 035301 (2014).
[13] E. Altman, E. Demler, and M. D. Lukin, Phys. Rev. A **70**, 013603 (2004).
[14] Those regimes have also been identified in [3], where the integral of the two-body correlation function is investigated.
[15] A. Perrin, R. Bücker, S. Manz, T. Betz, C. Koller, T. Plisson, T. Schumm, and J. Schmiedmayer, Nat. Phys. **8**, 195 (2012).
[16] A. Imambekov, I. E. Mazets, D. S. Petrov, V. Gritsev, S. Manz, S. Hofferberth, T. Schumm, E. Demler, and J. Schmiedmayer, Phys. Rev. A **80**, 033604 (2009).
[17] T. Langen, S. Erne, R. Geiger, B. Rauer, T. Schweigler, M. Kuhnert, W. Rohringer, I. E. Mazets, T. Gasenzer, and J. Schmiedmayer, Science **348**, 207 (2015).
[18] J.-C. Jaskula, G. B. Partridge, M. Bonneau, R. Lopes, J. Ruaudel, D. Boiron, and C. I. Westbrook, Phys. Rev. Lett. **109**, 220401 (2012).
[19] I. Bouchoule, K. V. Kheruntsyan, and G. V. Shlyapnikov, Phys. Rev. A **75**, 031606 (2007).
[20] I. Bouchoule, M. Arzamasovs, K. V. Kheruntsyan, and D. M. Gangardt, Phys. Rev. A **86**, 033626 (2012).
[21] L. Mathey, A. Vishwanath, and E. Altman, Phys. Rev. A **79**, 013609 (2009).
[22] T. Jacqmin, B. Fang, T. Berrada, T. Roscilde, and I. Bouchoule, Phys. Rev. A **86**, 043626 (2012).
[23] I. Shvarchuck, Ch. Buggle, D. S. Petrov, K. Dieckmann, M. Zielonkowski, M. Kemmann, T. G. Tiecke, W. von Klitzing, G. V. Shlyapnikov, and J. T. M. Walraven, Phys. Rev. Lett. **89**, 270404 (2002).
[24] M. J. Davis, P. B. Blakie, A. H. van Amerongen, N. J. van Druten, and K. V. Kheruntsyan, Phys. Rev. A **85**, 031604 (2012).
[25] See Supplemental Material at http://link.aps.org/supplemental/10.1103/PhysRevLett.116.050402, which includes Refs. [26,27], for further discussions of (1) the focusing technique to measure the momentum distribution; (2) the detailed calculations of the momentum correlation functions; (3) the detailed calculations of the $C$ function; (4) the temperature measurements of the experimental data; (5) the effect of normalization of the momentum distribution on noise correlations; and (6) a comparison with Bogolyubov theory for 1D condensates.
[26] S. Richard, F. Gerbier, J. H. Thywissen, M. Hugbart, P. Bouyer, and A. Aspect, Phys. Rev. Lett. **91**, 010405 (2003).
[27] J.-B. Trebbia, C. L. Garrido Alzar, R. Cornelussen, C. I. Westbrook, and I. Bouchoule, Phys. Rev. Lett. **98**, 263201 (2007).
[28] The resolution is estimated by fitting the cuts of the measured correlations of data A (IBG) in the direction where $p + p' =$ constant (i.e., parallel to the antidiagonal) and the correlations between different pixels are introduced by the imaging resolution alone (see discussions on IBG).
[29] The off-diagonal contributions may be due to the spurious effect induced by the large atom-number fluctuations in this low-density regime.
[30] The effect of a harmonic potential can be computed exactly for an IBG, but we prefer to adopt the LDA, which is a more general approach that is applicable to interacting gases, regardless of the shape of the external confinement.
[31] We have $\Delta \gg \hbar/L$, such that the bunching term introduces negligible correlations between different pixels.
[32] J. Esteve, J.-B. Trebbia, T. Schumm, A. Aspect, C. I. Westbrook, and I. Bouchoule, Phys. Rev. Lett. **96**, 130403 (2006).
[33] The correlation length in a finite-$T$ QBEC is given by $l_\phi$ (the first-order correlation function decreases as $e^{-|z|/(2l_\phi)}$) and $l_\phi/L = 0.035$, where $L$ is the FWHM of the cloud, and $l_\phi$ is evaluated at the center of the cloud.
[34] The measured fluctuations might also be due to jittering of the kicking potential used for focusing.
[35] For typical experimental parameters, the interactions in our system are not sufficiently weak for the mean-field predictions to be accurate [22]. We therefore refrain from using a classical field approach, as done in [20].
[36] O. F. Syljuåsen, Phys. Rev. E **67**, 046701 (2003).
[37] The regular part of the momentum correlation cancels almost completely the bunching on the diagonal.
[38] Note that the numerical computation of $C$ is, however, beyond the precision of our QMC calculations, mainly as a consequence of the coarse resolution of the measurements.
[39] S. Finazzi and I. Carusotto, Phys. Rev. A **90**, 033607 (2014).